Clinically visible progression indicators in age-related macular degeneration are transdifferentiated retinal pigment epithelium

Dongfeng Cao PhD, Belinda Leong MD, Jeffrey D. Messinger DC, Deepayan Kar MS, Thomas Ach MD, Lawrence A. Yannuzzi MD, K. Bailey Freund MD, Christine A. Curcio PhD

Corresponding author. Email: christinecurcio@uabmc.edu

SUPPLEMENTARY MATERIALS

LIST of SUPPLEMENTARY FIGURES

LIST of SUPPLEMENTARY TABLES

Supplementary figures

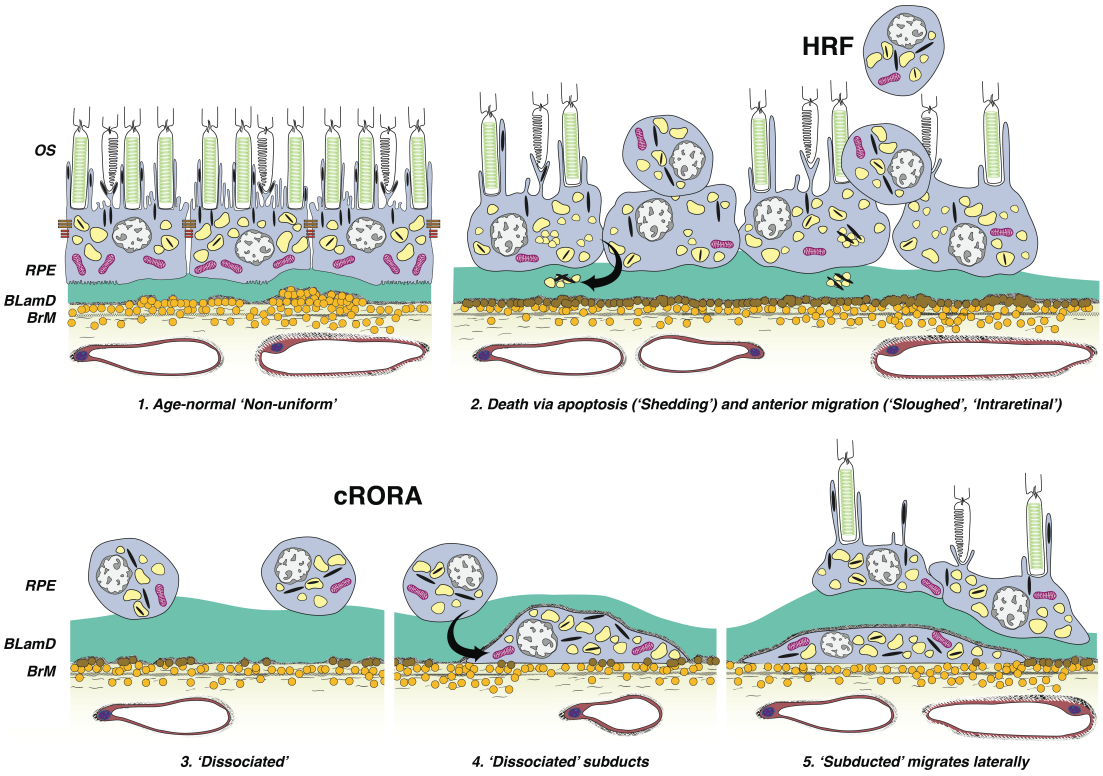

Fig. S1. a path from hyperreflective foci (HRF) to complete retinal pigment epithelium (RPE) and outer retinal atrophy (cRORA) in AMD.

cRORA is a multilayer definition of atrophy for OCT (*12*). Six morphologic phenotypes of RPE from a system of 15 (*25*) are shown. Schematic applies to non-neovascular AMD only. (**1)** Age-normal "nonuniform" RPE overlies Bruch's membrane (BrM), which has abundant lipoprotein particles (yellow). Basal laminar deposit (BLamD, green) is thickened basement membrane material between the RPE cell body and native RPE basal lamina. RPE organelles from apical to basal are melanosomes (black), lipofuscin (yellow), and mitochondria (pink) (*9*). Of overlying neurosensory retina, only photoreceptor outer segments are shown. (**2)** Anteriorly migrated RPE ("sloughed" and "intraretinal") manifest clinically as HRF. "Shedding" cells release organelle clusters (arrow, granule aggregates) basally into BLamD and can be visible in OCT. (**3)** Due to

cell death and migration, the RPE layer disintegrates. “Dissociated” RPE are fully pigmented, nucleated cells scattered in the atrophic zone that are eventually cleared. BLamD persists after RPE death then is also cleared. (**4)** “Subducted” cells containing RPE organelles are flattened against BrM, appearing to originate from Dissociated cells (arrow). **5.** “Subducted” cells migrate outside the atrophic area.

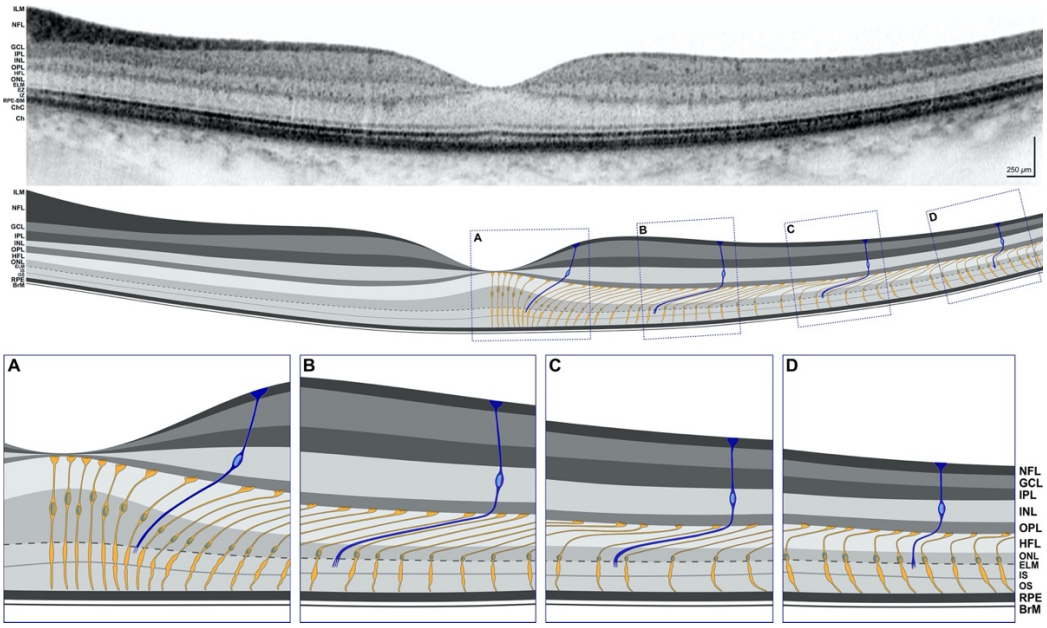

Fig. S2. Henle fibers in the human macula.

Top: Foveal OCT B-scan of a healthy female aged between 66 and 70 years demonstrating reflective bands corresponding to retinal layers. *Middle:* Schematized OCT scan shows cone photoreceptors *(yellow)* and Müller glia (blue). Müller glia span the retina, terminating at the external limiting membrane; for clarity, their branches in plexiform layers are omitted. The Henle fiber layer, shown in light gray, is visible in the original scan, especially under the fovea. *Bottom:* (**A)** At the foveal center, Henle fibers are short and perpendicular. *(***B)** In the parafovea, Henle fibers are long and oblique. (**C)** In the perifovea, Henle fibers gradually shorten. (**D)** At the macula edge, Henle fibers are very short and nearly vertical. Henle fibers are not present elsewhere in the retina. Schematic of B-scan was prepared (Illustrator, version 23.0.3, Adobe Inc., San Jose, CA) from an OCT B-scan (Spectralis, Heidelberg Engineering, Germany). Schematic of cellular trajectories was prepared in reference to a histological section of a donor eye (female, 76-80 years) immuno-labeled for glial fibrillary acidic protein in Müller glia (*87*).

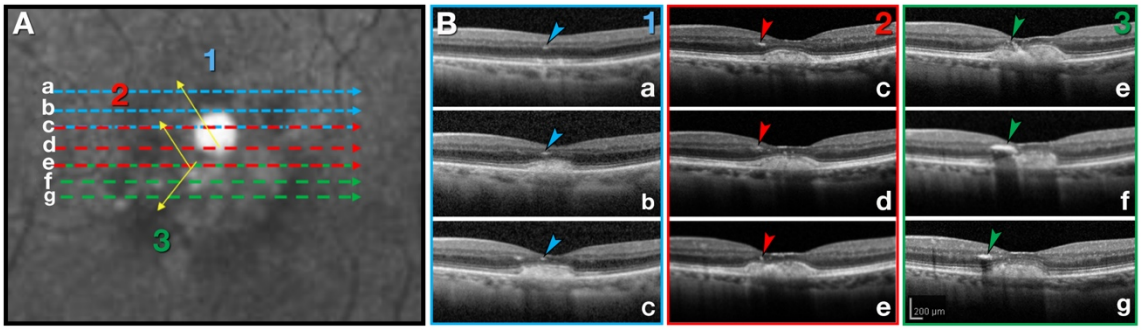

Fig. S3. Retinal pigment epithelium plumes exhibit directionality.

RPE plumes radiate outward from the fovea and thus may track as small reflective features across sequential horizontally oriented optical coherence tomography B-scans. **A.** Near-infrared reflectance (NIR) image shows plumes 1-3, with arrows indicating plume direction into the retina. Dashed lines (blue, red, green) correspond to scan lines a-g in panel B1-3. Positions of plumes, which are not visible in NIR, were assigned to this image and corresponded to the B-scans with the device software. **B.** Blue, red and green arrowheads indicate plumes 1-3, transected by each B-scan. In B1-c, a second plume is visible in addition to tracked plume 1. Scale bar in g applies to all panels of B.

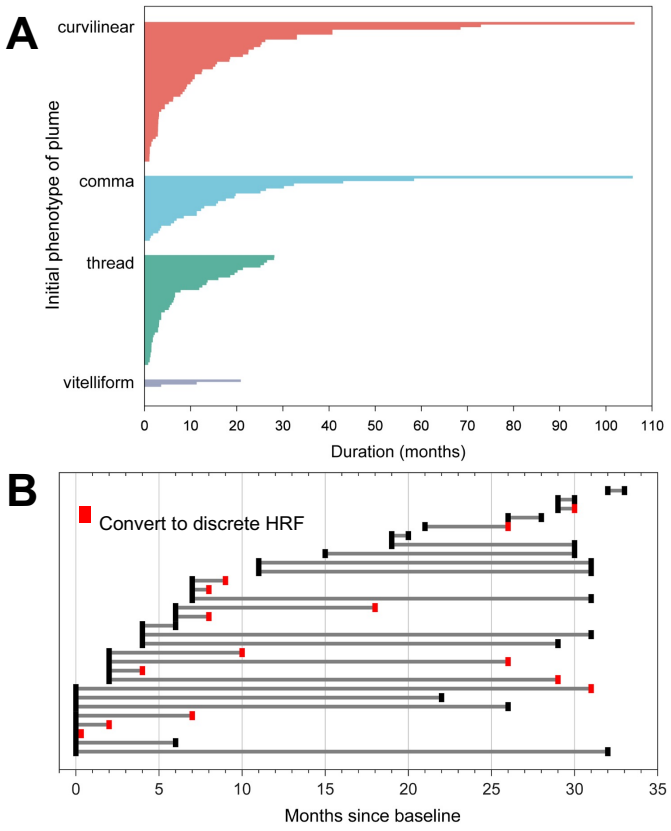

Fig. S4: Duration and evolution of plumes.

(A) Duration of each of 129 plumes, stratified by morphology, and displayed in descending order of duration. The longest lasting plumes were curvilinear and comma. (**B)** Each plume in one eye with the most plumes represented as a single horizontal line. Duration is shown, with conversion to discrete HRF, no longer associated with the RPE, indicated; representative of data from 3 eyes.

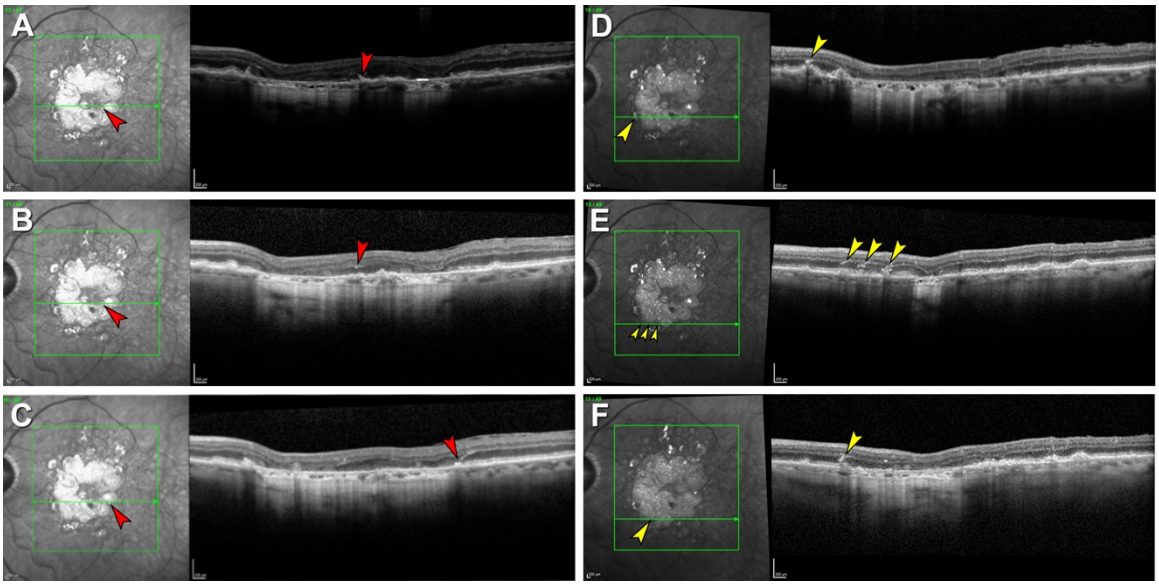

Fig. S5. Variations in RPE plume trajectory in atrophy.

Plumes located along the border of complete RPE and outer retinal atrophy (cRORA, (*12*)) are indicated in the near infrared reflectance images at the left of each panel. Green lines indicate areas covered by OCT volumes and locations of individual B-scans in A-F. (**A** and **B)** Posterior (A) and anterior (B) components of a plume (red arrowheads) traversing radially away from the fovea, i.e., congruent with the HFL. (**C)** Another plume (red arrowhead) is congruent with the normal HFL, adjacent to a hyporeflective wedge (*88*). (**D** to **F)** Examples of plumes traversing anteriorly in the opposite direction, i.e., non-congruent with the normal HFL (yellow arrowheads), near the border of atrophy, possibly due to subsidence (sinking) of outer retinal layers in atrophy.

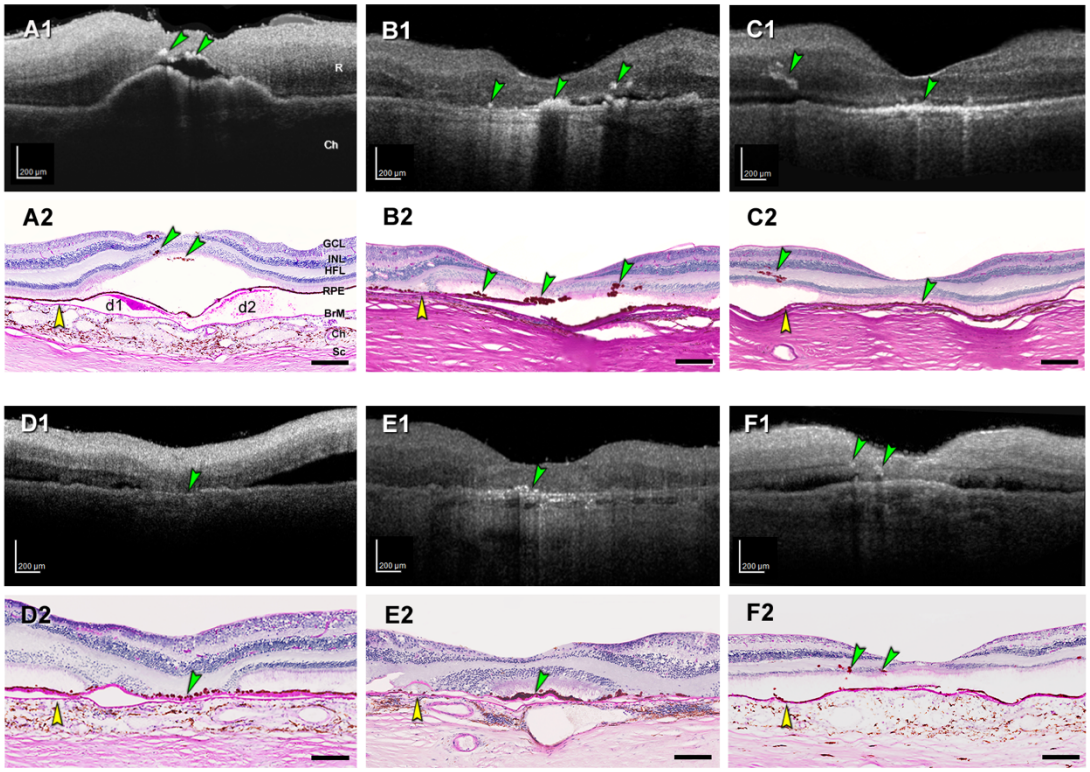

104

105 ***Fig. S6. HRF in ex vivo OCT match intraretinal RPE on histology.***

106 Reflective features including hyperreflective foci (HRF) are visible in donor eyes
107 (numbers in table S5 by *ex vivo* optical coherence tomography (A1 to F1). These were
108 matched with RPE phenotypes in histology sections stained with periodic acid Schiff
109 hematoxylin (PASH) (A2 to F2), to show Bruch's membrane (BrM), basal laminar
110 deposit, and drusen. In all panels, scale bars are 200 µm; yellow arrowheads indicate
111 BrM, and green arrowheads indicate HRF in OCT and ectopic RPE in histology. (**A1** and
112 **A2)** HRFs above soft drusen at fovea from early-intermediate AMD eye (#5). (**B1** and
113 **B2)** HRFs at the fovea and nasal and temporal side, from atrophic AMD eye (#17). (**C1**
114 and **C2)** RPE plume in atrophic AMD eye (#15). (**D1** and **D2**) Hyperreflective dots in
115 OCT and dissociated RPE atop thick BLamD in the atrophic area. (**E1** and **E2**) Reflective
116 dots under an island of surviving photoreceptors in the fovea center of an atrophic AMD

eye (#12). (**F1** and **F2**) Multiple HRFs nasal to the fovea in an early-intermediate AMD eye, corresponding to intraretinal RPE cells (#7).

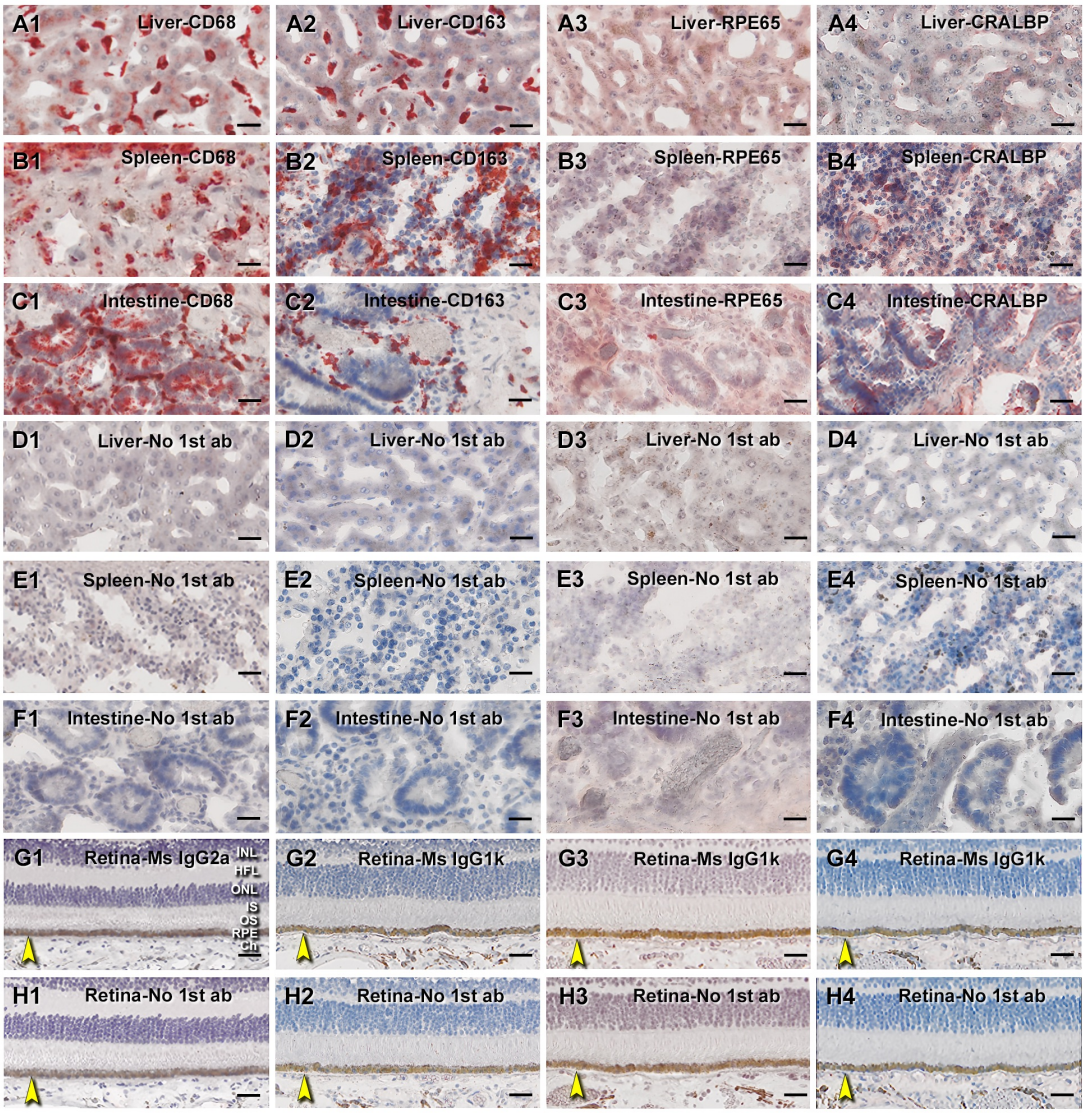

121

122 ***Fig. S7. Positive and negative controls for immunohistochemistry.***

123 A cryosection of human tissue array with liver, spleen, and intestine tissue made in-
124 house was used as positive and negative controls for immunohistochemistry studies with
125 antibodies to CD68, CD163, RPE65, and CRALBP (positive A to C, negative D to H).
126 Human retinal sections from an unremarkable eye (#3, table S5) was used for isotype
127 and sham controls. BrM was pointed by yellow arrows. Scale bars are 20 μm for non-
128 retinal tissues and 50 μm for retina. (**A1** to **A4)** CD68+, CD163+, RPE65-, and CRALBP-

Kupffer cells in liver tissue. **(B1** to **B4)** CD68+, CD163+, RPE65-, and CRALBP+ red pulp cells in spleen tissue. **(C1** to **C4)** CD68+, CD163+, RPE65+, and CRALBP+ cells in intestine tissue. **(D1** to **D4)** Liver sham controls. **(E1** to **E4)** Spleen sham controls. **(F1** to **F4)** Intestine sham controls. **(G1** to **G4)** Retina isotype controls with mouse IgG2a for CD68 and mouse IgG1k for CD163, RPE65, and CRALBP. **(H1** to **H4)** Retina sham controls for CD65, CD163, RPE65, and CRALBP. All human tissue sections have CD68 and CD163 immunoreactivities and uncertain RPE65 and CRALBP immunoreactivities. All isotype and sham controls omitting primary antibodies control are negative.

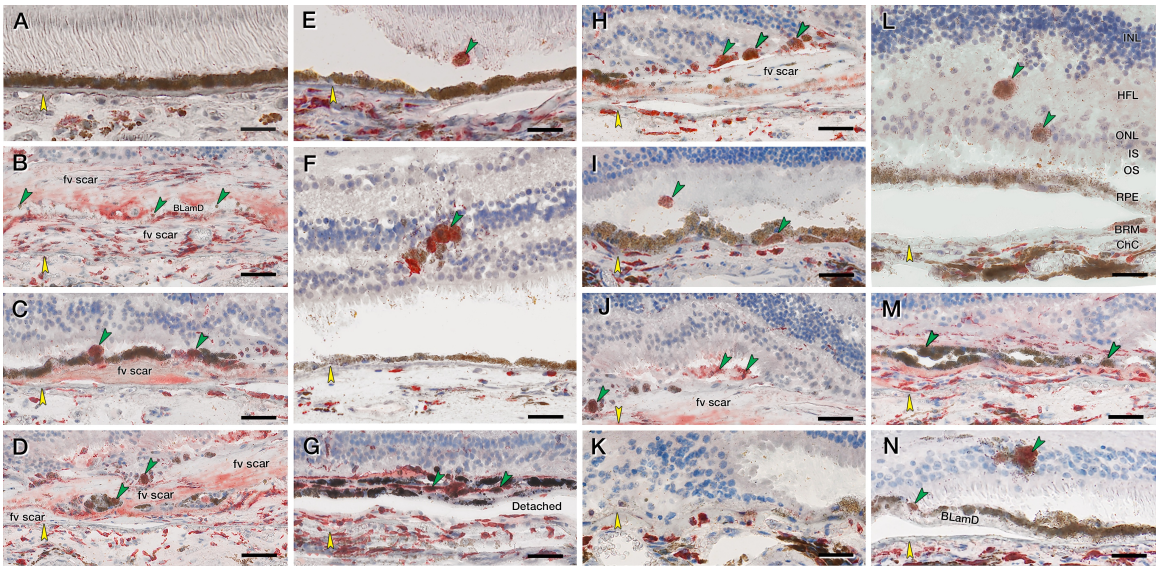

Fig. S8. RPE corresponding to HRF and other abnormal cells are CD163+.

Twenty donor eyes (16 AMD, 4 control; eye number in table S5) were used for immunohistochemistry with mouse monoclonal anti-human CD163 (table S6). Fourteen of 16 previously described morphologic phenotypes of RPE were identified (table S7). All scale bars are 20 μm; yellow arrowheads indicate BrM, and green arrowheads indicate abnormal RPE phenotypes. (**A**) CD163- "Uniform" RPE, unremarkable (#1). (**B**) CD163- ''Shedding'' RPE, nvAMD (#20). (**C**) CD163+ ''Sloughed'', nvAMD (#20). (**D**) Both CD163+ and CD163- are present in ''Entombed'' RPE, nvAMD (#20). (**E**) A single CD163+migrating RPE above "Nonuniform" RPE layer, atrophic AMD (#17). (**F**) CD163+ ''Intraretinal'' RPE, atrophic AMD (#15). (**G**) Variable CD163 immunoreactivities in ''Melanotic'' RPE, nvAMD (#20). (**H**) CD163+ "Severe" or "Very nonuniform" RPE, nvAMD (#20). (**I**) CD163+ ''Subducted'' and "Sloughed" RPE, atrophic AMD (#16). (**J**) CD163+ ''Entubulated'' and "Dissociated" RPE, nvAMD (#20). (**K**) There is no RPE in an area of ''Atrophy without BLamD'', atrophic AMD (#16). (**L**) CD163+ "Dissociated" and "Intraretinal" RPE, atrophic AMD (#16). (**M**) Variable CD163 immunoreactivity in

155 ‘‘Bilaminar’’ RPE, nAMD (#20). (**N**) CD163+ “Intraretinal“ RPE at ‘‘Atrophy with BLamD’’

156 area, atrophic AMD (#14).

157

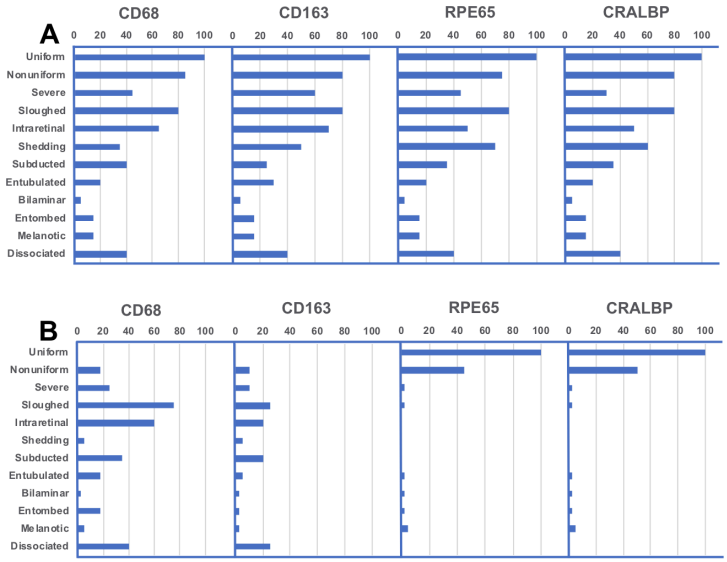

Fig. S9. Gain- and loss-of-function of RPE and RPE-derived cells.

(**A**) The distribution of phenotypes (vertical axis) was similar across the sections used for immunohistochemistry for retinoid markers RPE65 and CRALBP and immune markers CD68 and CD163 (at top of graphs). Uniform and Non-uniform phenotypes are age-normal. Of the others, Entubulated and Subducted are found in geographic atrophy and neovascular AMD, Melanotic is found only in neovascular AMD, and others are found at all AMD diagnostic stages. Vitelliform and Vacuolated are not shown due to small numbers in the current sample. (**B**) Bar lengths represent the percentage labelled (scoring with 0-not labelled, 1-some labelled, and 2-all abnormal cells labelled; total scores/ maximum possible score = 40 x 100) by CD68, CD163, RPE65 and CRALBP. Age-normal uniform cells are strongly labelled by retinoid markers and are not labelled by immune markers. Non-uniform cells exhibit a reduced proportion of retinoid markers and a small proportion of immune markers. Phenotypes below “severely non-uniform” on the vertical axis are considered abnormal. These are labeled for immune markers and

minimally labelled for retinoid markers (<5%), especially “Sloughed” and “Intraretinal” morphologies corresponding to HRF in OCT.

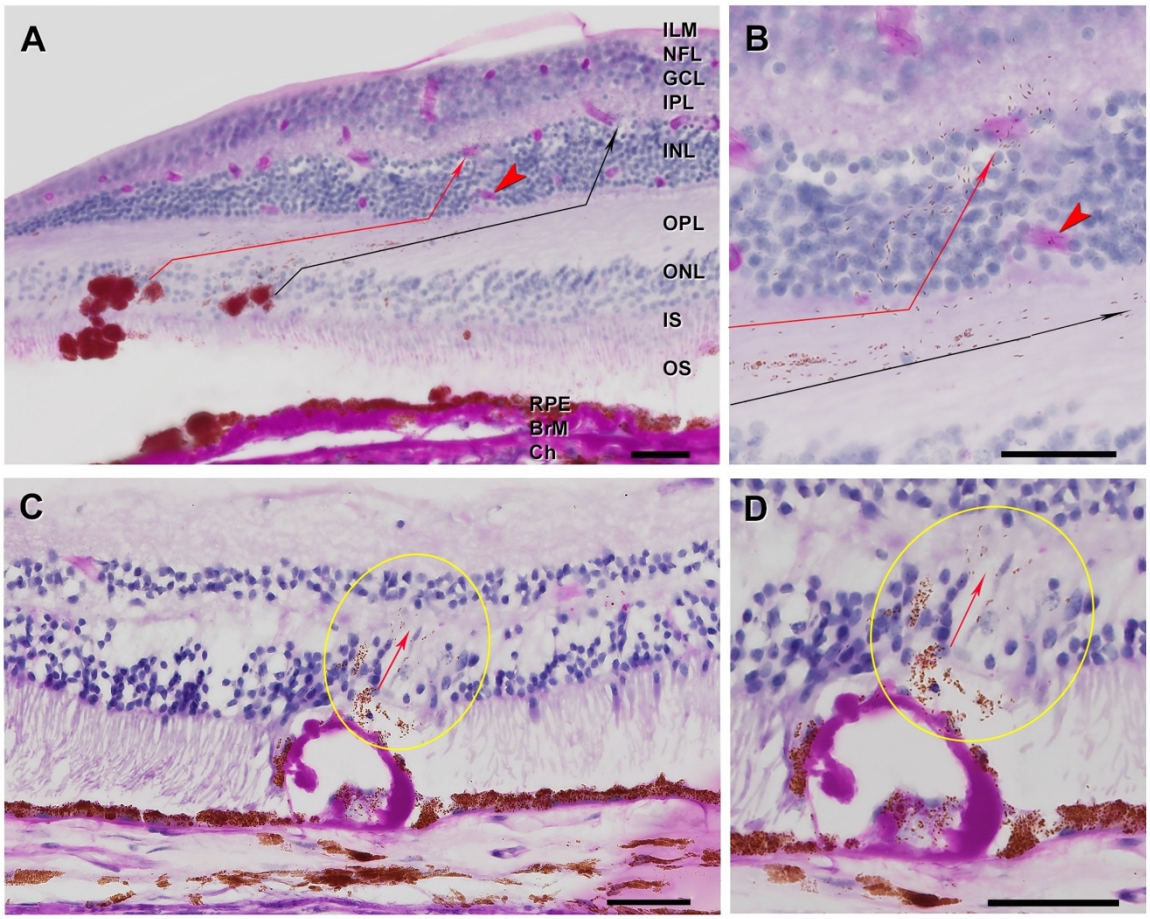

Fig. S10. Dispersing melanosomes follow regionally specific trajectories of Müller glia.

A and **B**, donor aged 96-100 years (#17, table S5). **C** and **D**, donor aged 81-85 years (#1, table S5). All scale bars are 50 μm. Cryosection, periodic acid Schiff hematoxylin stain. (**A** and **B)** In the macula RPE detritus follows the obliquely oriented HFL fibers and crosses vertically into the INL. Thin red and black arrows indicate detritus emanating from two groups of cells in the ONL. (**C** and **D)** In the periphery where HFL is absent, RPE organelles enter vertically retina directly above an artifactually empty druse lined by BLamD and lacking overlying RPE.

Supplementary tables

Table S1. Demographics of clinic patients

Variable (SD, standard deviation)	**Value**
Number of patients	44
Number of eyes	61
Age, mean ± standard deviation (years)	79.4 ± 7.7
Gender: Female, N (%)	29 (47.5)
Eyes with RPE plume	29 (47.5)
Follow-up duration (years, per individual eyes)	4.7 ± 0.09
Total number of plumes	129
Plumes/eye (range, SD)	4.0 (1-30, 5.9)
Distance in µm, fovea to plume center, mean (SD); range	1555 (SD 876); 0 – 3558
Presence of AMD features: N (%)	
Soft drusen only	10 (16.4)
Cuticular drusen only	8 (13.1)
Mixed drusen types	34 (55.7)
Drusenoid pigment epithelial detachment*	27 (44.3)
Complete RPE and outer retinal atrophy**	29 (47.5)
*≥350 µm greatest linear diameter (*89*) **cRORA as defined (*12*)	

192 ***Table S2. Plume disposition at final visit***

Fates of 129 individual plumes (baseline vs final)	**# (% of 129)**
Complete resolution *with conversion* to another plume morphology or discrete HRF	38 (29.5)
Complete resolution *without conversion* to another plume morphology or discrete HRF	36 (27.9)
Unresolved *with conversion* to another plume morphology or discrete HRF	35 (27.1)
Unresolved *without conversion* to another plume morphology or discrete HRF	20 (15.5)
Total	**129 (100)**

193

194

Table S3. Plume trajectory relative to HFL and macular quadrant

	Congruent With normal HFL		Non-congruent With normal HFL	
	# eyes	**# plumes**	**# eyes**	**# plumes**
Curvilinear	17	42	7	15
Comma	14	19	2	6
Thread	12	36	5	7
Vitelliform	3	4	0	0
Superior temporal	13	34	0	0
Superior nasal	15	23	4	19
Inferior nasal	9	18	2	5
Inferior temporal	17	26	3	4

199 ***Table S4. Plume association with atrophy***

Association with atrophy (at final visit)	**# (% of 129 total)**
Associated with cRORA	73 (56.6)
Congruent	48 (37.2)
Incongruent	25 (19.4)
At cRORA border	16 (12.4)
Associated with iRORA	6 (4.7)
Congruent	6 (4.7)
Incongruent	0 (0)
Not associated with cRORA or iRORA	50 (38.8)
Total	**129**
cRORA, complete RPE and outer retinal atrophy; iRORA, incomplete RPE and outer retinal atrophy (*5, 12*) Congruent, incongruent; relative to trajectory of normal HFL at that location	

200

201

202 ***Table S5. Characteristics of donor eyes***

Order	Age range	Sex	D-P, hours	Histologic diagnosis
1	81-85	M	4.05	Unremarkable
2	86-90	F	5.48	Unremarkable
3	76-80	F	4.82	Unremarkable
4	91-95	F	3.75	Unremarkable
5	86-90	F	4.75	Early-intermediate AMD
6	86-90	F	3.25	Early-intermediate AMD
7	91-95	M	3.63	Early-intermediate AMD
8	86-90	F	4.95	Early-intermediate AMD
9	81-85	F	3.58	Early-intermediate AMD
10	96-100	F	3.98	Early-intermediate AMD
11	96-100	F	3.12	Early-intermediate AMD
12	91-95	M	3.45	Atrophic AMD
13	91-95	F	3.78	Atrophic AMD
14	81-85	F	3.50	Atrophic AMD
15	86-90	F	3.42	Atrophic AMD
16	86-90	M	4.15	Atrophic AMD
17	96-100	F	2.33	Atrophic AMD
18	86-90	F	3.50	Neovascular AMD
19	91-95	F	4.15	Neovascular AMD
20	86-90	F	3.80	Neovascular AMD

Notes:
Total 20 eyes of 20 white donors. Age ranges in years: 76-80; 81-85; 86-90; 91-95; 96-100; mean age 89.2 ± 5.0 years; 4 males and 16 females. D-P, death to processing time in hours; mean D-P 3.87 ± 0.72 hours; 4 unremarkable, 7 early-intermediate AMD, 6 atrophy AMD, 3 neovascular AMD.

203

Table S6: Antibodies used

Antibody Name	Clone #	Cat#	Lot#	Isotype	Dilution	Vendor Web Link
CD68 Monoclonal	514H12	MA1-80133	C2619	Mouse IgG 2a	1:100	https://www.fishersci.com/shop/products/anti-cd68-clone-514h12/ma180133
CD163 Monoclonal	10D6	MA5-11458	D1118	Mouse IgG 1	1:100	https://www.fishersci.com/shop/products/anti-cd163-clone-10d6-thermo-scientific-pierce/pima511458
RPE65 Monoclonal	401.8B11.3D9	MA1-16578	UE2776581	Mouse IgG 1k	1:150	https://www.fishersci.com/shop/products/anti-rpe65-clone-401-8b11-3d9/ampa6578
CRALBP Monoclonal	B2	MA1-813	UB272117	Mouse IgG 1	1:500	https://www.fishersci.com/shop/products/anti-cralbp-clone-b2/ma1813#
Mouse IgG 2a	PPV-04	MA1-10418	UC282768	Mouse IgG 2a	1:1000	https://www.fishersci.com/shop/products/mouse-igg2a-clone-ppv-04-isotype-control-thermo-scientific-pierce/pima110418
Mouse IgG 1Kappa	P3.6.2.8.1	14-4714-82	1957953	Mouse IgG 1k	RTU	https://www.fishersci.com/shop/products/igg1-k-mouse-clone-p3-6-2-8-1-isotype-control-ebioscience-3/501129668
Horse anti-Mouse Biotin	NA	PK-7200	ZE0720	Horse IgG	RTU	https://vectorlabs.com/catalogsearch/result/?q=pk-7200
RTU, ready to use						

Table S7: Morphologic phenotypes of RPE and its basal lamina in AMD

Name	Attached to basal lamina	Description (in toluidine-blue stained sub-micrometer sections of osmium-tannic-acid paraphenylenediamine post-fixed human eyes)
Uniform	Yes	Uniform height and pigmentation; hexagonal
Non uniform	Yes	Slightly non-uniform morphology and pigmentation; hexagonal
Very non uniform	Yes	Very non-uniform morphology and pigmentation
Sloughed	No	Continuous epithelium with equally pigmented spherical cells sloughed into sub-retinal space
Shedding	Yes	Continuous epithelium with groups of organelles (non-nucleated, non-membrane bound) shed into thick underlying basal laminar deposits; granule aggregates form in the cell bodies.
Bilaminar	Yes	Double layers; usually neovascular AMD
Vacuolated	Yes	A single large vacuole, sometimes with contents, delimited apically by extremely effaced cytoplasm (rare)
Intraretinal	No	Anterior migration of nucleated and pigmented cells, singly and in groups, through the external limiting membrane; mostly spherical, some amoeboid
Vitelliform	No	Massively liberated RPE organelles in the subretinal space
Dissociated	No	Spherical cells in scattered in atrophic areas, usually adherent to persistent BLamD.
Entombed	Yes	Entombed by fibrovascular scar in neovascular AMD, intermingled with other cells and fluid in the same layer
Subducted	No	Rounded or flattened, in sub-RPE-basal laminar space, with varying numbers of RPE-characteristic organelles
Melanotic	Yes	Single or multiple cells in layers with black spherical melanosomes, some large (up to 5 μm diameter), in sub-retinal or sub-RPE space; neovascular AMD only
Entubulated	No	In lumen of outer retinal tubulation (tubes of photoreceptors, mainly cones, scrolled by Müller glia)
Atrophy with BLamD	No	No RPE, persistent basal laminar deposits
Atrophy without BLamD	No	No RPE, no basal laminar deposit (retina consists of gliotic Müller cells in contact with inner collagenous layer of Bruch's membrane
Phenotypes defined using 1-μm-thick epoxy resin sections of osmium-tannic-acid paraphenylenediamine post-fixed human eyes with AMD, stained with toluidine blue, referenced to previously published AMD morphology (*18, 19, 25*). All cells except where noted are		

nucleated and have abundant lipofuscin, melanolipofuscin, and characteristic spindle-shaped melanosomes in the cell bodies. Melanosomes are abundant in apical processes (*9*), which may be lost due to disease or to artifactual detachment of photoreceptors from RPE or both. Lipofuscin and melanolipofuscin are ovoid (~1 μm in diameter), densely packed, and green-bronze-olive color in toluidine blue stain, depending on the specimen. Cell morphologies recognized in this preparation are readily identified in the cryosections used in this study. Granule aggregates (Shedding phenotype) are also visible in RPE cell bodies by fluorescence microscopy (*36*). Vitelliform (*90*) is under active investigation (*45*) and was not identified in the current series but is included for completeness.